

Article

Icephobic Coating Based on Epoxy/Polydimethylsiloxane Interpenetrating Polymer Network Gel

Lin Zhao ¹, Tianhui Hao ¹, Qiang Xie ², Yuan Tian ¹ , Jifeng Zhang ¹  and Haotian Guo ^{1,*}

¹ Intelligent Structure and Advanced Composite Materials Lab., College of Aerospace and Civil Engineering, Harbin Engineering University, Harbin 150001, China; zlz1@hrbeu.edu.cn (L.Z.); haotianhui@hrbeu.edu.cn (T.H.); tian_yuan@hrbeu.edu.cn (Y.T.); jfzhang@hrbeu.edu.cn (J.Z.)

² Aero Engine Corporation of China Sichuan Gas Turbine Research Institute, Chengdu 610500, China; xieqiang62420@163.com

* Correspondence: guohaotian@hrbeu.edu.cn

Abstract: Ice accretion endangers the safety and reliability of equipment operation in frigid regions. Silicone polymer icephobic coatings present themselves as an effective strategy. However, they face durability challenges, which is a crucial foundation for expanding their application. In this work, a durable icephobic coating was prepared based on an epoxy/polydimethylsiloxane (PDMS) interpenetrating polymer network (IPN) gel. In the process, epoxy was used to improve mechanical performance. IPN technology was used to integrate PDMS and epoxy. Low-molecular-weight silicone oil was used to adjust the elastic modulus of the coating by reducing crosslinking. The mechanical properties, icephobicity and durability of the coatings were characterized through elastic modulus measurements, ice adhesion strength tests, and icing/deicing cycle tests, respectively. Results shows the ice adhesion strength of the epoxy/PDMS IPN gel coating was approximately 8 kPa when the elastic modulus was 0.18 MPa. Additionally, the epoxy/PDMS IPN gel has good durability, weather resistance, and substrate adhesion. After 25 icing/deicing cycle tests, the coating remained undamaged, and the ice adhesion strength was stable in the range of 3–14 kPa. Within the range of –5 to –30 °C, the ice adhesion strength of the coating was stable and less than 20 kPa. After 168 h of salt spray aging test, the ice adhesion strength of the coating was maintained at 48.72 ± 5.27 kPa. This can provide a reference for an icephobic coating design.

Keywords: icephobic coating; interpenetrating polymer network; organogel; elastic modulus; epoxy; polydimethylsiloxane



Citation: Zhao, L.; Hao, T.; Xie, Q.; Tian, Y.; Zhang, J.; Guo, H. Icephobic Coating Based on Epoxy/Polydimethylsiloxane Interpenetrating Polymer Network Gel. *Coatings* **2024**, *14*, 76. <https://doi.org/10.3390/coatings14010076>

Academic Editors: Łukasz Gierz, Mariola Robakowska and Paulina Paulina Mayer

Received: 28 November 2023

Revised: 30 December 2023

Accepted: 3 January 2024

Published: 5 January 2024



Copyright: © 2024 by the authors. Licensee MDPI, Basel, Switzerland. This article is an open access article distributed under the terms and conditions of the Creative Commons Attribution (CC BY) license (<https://creativecommons.org/licenses/by/4.0/>).

1. Introduction

Ice accretion has negatively impacted production and life, leading to catastrophic consequences in road transportation, the power industry, aerospace, wind power, ships, and ocean platforms [1–3]. While researchers have had many discussions about how to repel water before it can form ice and have made some progress, only delayed freezing has been achieved [4,5]. Complete prevention of ice accretion in extreme conditions is still considered a challenge [6,7]. This emphasizes the importance of easily removing ice [8]. Icephobic coating, defined as having an ice adhesion strength below 100 kPa [9,10], has received widespread attention from researchers due to its environmental, economic, and energy-saving potential [11,12].

The design idea for an icephobic coating is to find a material that has long-term adhesion to a structural surface on one side and excellent icephobic properties on the other side [13]. For example, the ice adhesion strength of ice on a smooth aluminum alloy surface is approximately 727 ± 227 kPa [14]. By applying an icephobic coating to the aluminum alloy surface, the ice adhesion strength is reduced to less than 20 kPa, allowing ice to be easily removed by natural forces [15]. Silicone polymers and fluoropolymers exhibit low surface energies [16], making them candidates for icephobic coatings [17].

Liu et al. [18] prepared a coating with icephobic capability by combining low-surface-energy fluorosilicone resin with hydrophobic nano-SiO₂-poly (methyl-3,3,3-trifluoropropyl siloxane) particles. The coating surface exhibits an ice adhesion strength of only 34 kPa at −25 °C. After 10 icing/deicing cycles, the ice adhesion strength of the coating stabilized below 40 kPa. Wang et al. [19] prepared icephobic coatings from tetrahydrofuran (THF), glycerol triglycidyl ether (GTE) derived from natural glycerin and bis(3-aminopropyl)-terminated PDMS by a one-pot method. The THF-GTE-PDMS coating (molecular weight of PDMS is 5000) exhibits an ice adhesion strength of only 16 kPa, and after 20 icing/deicing cycles, the ice adhesion strength was similar to the initial test. Qi et al. [20] utilized silicone oil-swollen trimethyl-capped PDMS to create a low-modulus organic gel coating, which resulted in an ice adhesion strength of 6.5 kPa at −10 °C. Apparently, these studies were able to achieve significantly reduced ice adhesion strength by adjusting the surface properties of the coating. However, they encountered challenges with coating durability due to the inferior mechanical properties of silicone polymers and fluoropolymers [17,21].

On the other hand, while it is necessary to obtain durable coatings for wider applicability, it is also believed that the adjustment of mechanical properties can affect the adhesion strength of ice. According to interfacial fracture mechanics, M. Nosonovsky, He and Jiang et al. [22–24] found that the adhesion strength of ice (τ_{ice}) can be estimated by the following equation:

$$\tau_{ice} = \sqrt{\frac{EG}{\pi a \Lambda}} \quad (1)$$

where E is the elastic modulus, G is the surface energy, a is the length of the interface crack, and Λ is a non-dimensional constant determined by the geometric configuration of the crack. M.K. Chaudhury and Li et al. [25,26] also found that the critical shear stress τ_{ice} (e.g., ice adhesion strength) required to shear a rigid body (e.g., ice) from an elastic thin film is:

$$\tau_{ice} \propto \sqrt{\frac{WE}{t}} \quad (2)$$

where W is the work of adhesion, E is the elastic modulus of the film, and t is the thickness of the film. The above two equations indicate that lowering the surface energy and elastic modulus of a coating can effectively reduce the ice adhesion strength. Therefore, it is worth noting that an icephobic coating should not only meet the requirements of easy removal of ice accretions, but also be durable, weather resistant, and environmentally friendly [27]. In addition, the effect of changes in mechanical strength on icephobicity should be clarified [28].

In this paper, we designed an icephobic coating based on an epoxy/PDMS interpenetrating polymer network (IPN) gel. The role of the epoxy is to enhance the durability of the coating itself and the bond strength of the coating to the substrate. Low-molecular-weight silicone oil was added to reduce the modulus by decreasing the crosslink density. Using IPN technology, we integrated the incompatible epoxy and PDMS together. By combining IPN and the gelation process, uniform, low-modulus and durable epoxy/PDMS IPN gel coatings were obtained. The icephobic properties of gel coatings were determined by testing the adhesion of ice to the surface. This work also attempted to reveal the relationship between roughness, wettability, elastic modulus and icephobicity. In addition, the durability of the coatings was evaluated after icing/deicing cycle tests, deicing tests at different temperatures, X-cut coating adhesion tests and neutral salt spray aging tests.

2. Materials and Methods

2.1. Materials

PDMS (α , ω -dihydroxy-PDMS, type 107, viscosity: 5000 cps) was obtained from Jiangxi Silicon Bo Chemical Co., Ltd., Nanchang, China; Tetraethyl orthosilicate (TEOS), and cyclohexane was obtained from Tianjin Kemiou Chemical Reagent Co., Ltd., Tianjin, China; Di-n-butyltin dilaurate (DBTL) and sodium chloride were obtained from Sinopharm

Chemical Reagent Co., Ltd., Shanghai, China; Bisphenol A epoxy (type E-51, epoxy value: 0.48~0.54 eq/100 g, viscosity: 11,000 cps) was obtained from Wuxi BLUE-STAR Petrochemical, Wuxi, China; Polyether amine (PEA, type D230) was obtained from Changzhou Runxiang Chemical Co., Ltd., Changzhou, China; Silicone oil (PMX-200, 50 cs) was obtained from Dow Corning, Midland, MI, USA. All reagents were not further purified before use.

2.2. Preparation of the Epoxy/PDMS IPN Gel

Based on the idea of improving the durability and icephobic properties of PDMS coatings, we plan to design an epoxy-reinforced PDMS icephobic coating and investigate the effect of the mechanical properties of this coating on the ice adhesion strength. The specific preparation process is as follows. First, PDMS, cyclohexane (diluent, 500% by weight of PDMS), TEOS (crosslinking agent, 10% by weight of PDMS), epoxy (0%, 100%, and 200% by weight of PDMS), and silicone oil (0%, 50%, 100%, 150%, and 200% by weight of PDMS) were mixed in a beaker and then stirred at 500 rpm for 20 min using a magnetic rotor stirrer. DBTL (catalyst, 2% by weight of PDMS) and PEA (curing agent, 30% by weight of epoxy) were then added to the above beaker and stirred at 500 rpm for 2 min with a magnetic rotor stirrer until the mixture became homogeneous (epoxy/PDMS weight ratio is 0:1 (PDMS gel), 1:1, and 2:1).

The solution in the beaker was then aspirated into a syringe, and the epoxy/PDMS IPN gel coatings were prepared by the one-step spraying method using the FS650 ultrasonic atomization spraying machine as shown in Figure 1. The ultrasonic nozzle was set at 100 mm above the substrate, and the PDMS/epoxy mixture was uniformly sprayed onto the substrate (5 cm × 4 cm × 0.2 cm aluminum alloy) at a traveling speed of 30 mm/s. The substrates were ultrasonically cleaned in acetone and dried in an oven before use. The coated substrate was then placed on a heating platform at 80 °C for 3 h. After the diluent evaporated, the substrate was cured at room temperature for 24 h. Figure 2 shows a schematic representation of the epoxy/PDMS IPN gel formation. The thickness of all coatings was consistent as measured with electronic calipers. The thickness of all coatings was approximately 1 mm.

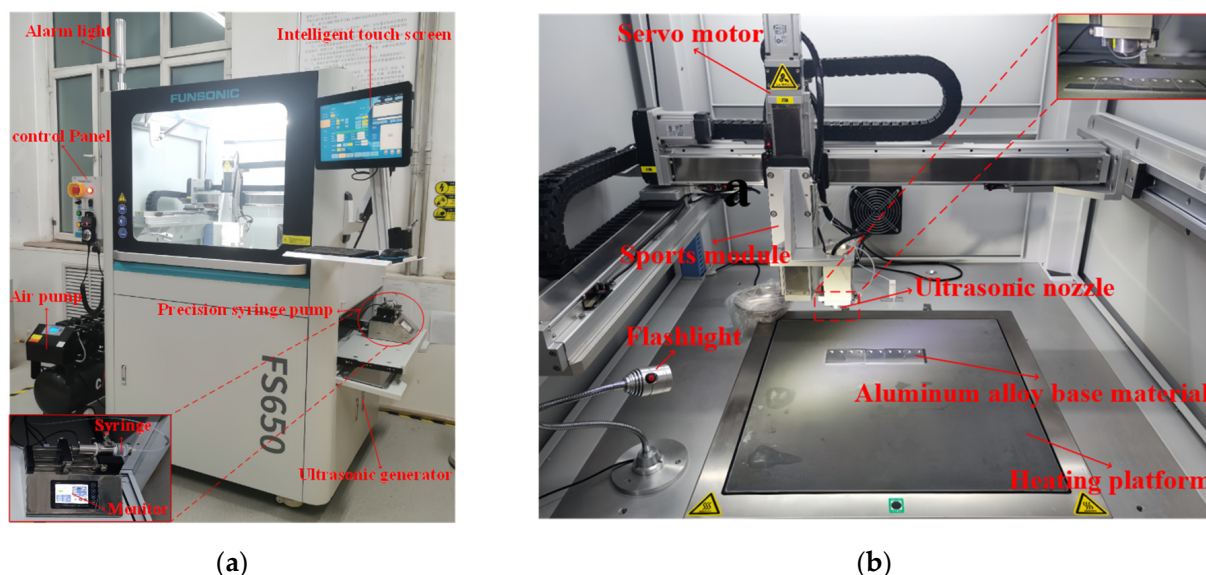


Figure 1. (a) Photograph of FS650 ultrasonic atomization spraying machine body and ISPLab Syringe Pump; (b) internal structure and spraying device of ultrasonic atomization spraying machine.

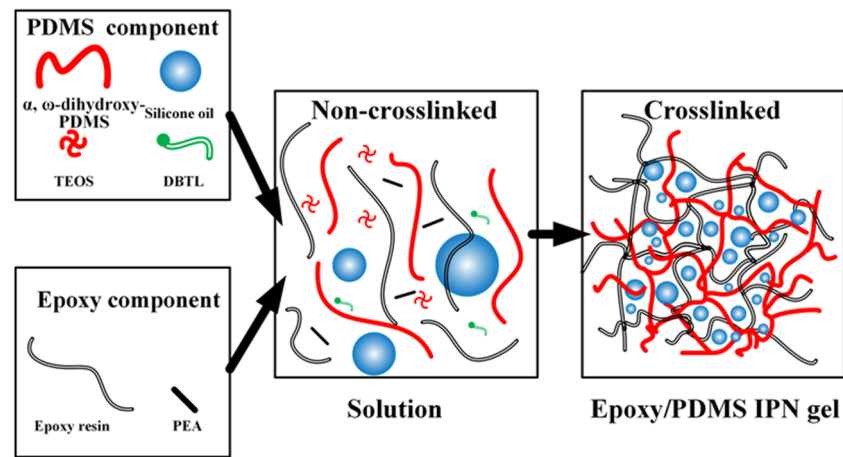


Figure 2. Schematic representation of the epoxy/PDMS IPN gel formation.

3. Characterization and Performance Measurement

The ice adhesion strength (τ_{ice}) was measured using a refrigerated centrifuge as shown in Figure 3a. First, a silicone mold with a cuboid cavity (25 mm × 25 mm × 15 mm) was filled with deionized water. Then, the coated substrate was placed upside down on the silicone mold and in full contact with the water. Next, they were frozen for 3 h at a desired temperature. After freezing, the substrate with ice was pulled out from the silicone mold and bolted to a rotor (radius is 150 mm) inside the refrigerated centrifuge (see Figure 3b). The inside temperature of the refrigerated centrifuge was set to the desired temperature for 30 min of heat preservation, and then the rotor was started. When the centrifugal force overcame τ_{ice} , the ice detached from the coating and impacted the protective net. At the same time, the rotation speed (rpm) was recorded. The τ_{ice} can be calculated by the centrifugal formulas: $\tau_{ice} = F/A$ and $F = mr\omega^2$, where τ_{ice} is the apparent ice adhesion strength (Pa), F is the centrifugal force (N), A is the iced area (m²), m is the mass of ice (kg), r is the distance from the ice centroid to the rotor center (m), and ω is the speed of rotation when the ice detached (rad/s, 1 rpm = $\pi/30$ rad/s). The same five samples were prepared for every coating to obtain the average and standard deviation of τ_{ice} .

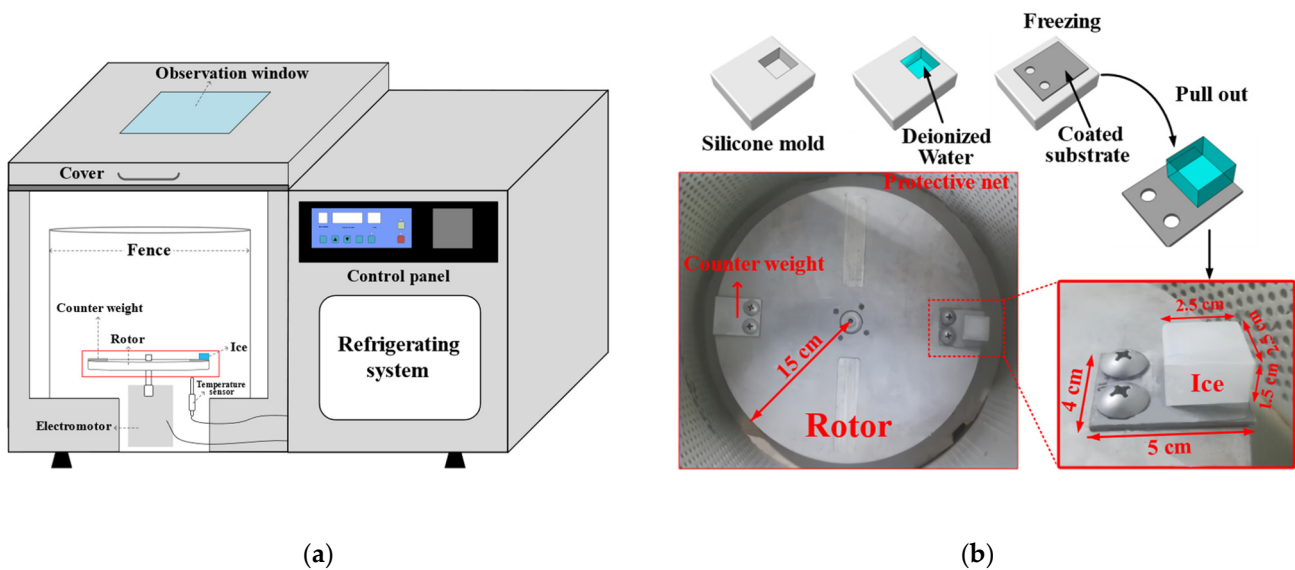


Figure 3. (a) Schematic diagram of the refrigerated centrifuge; (b) ice formation and centrifugal adhesion setup inside the refrigerated centrifuge.

The surface morphology of the IPN gel coating was obtained using an optical profilometer (Bruker ContourGT, Karlsruhe, Germany). The morphology images were de-noised by median filtering. Profile roughness parameters (R_a and R_q) and areal roughness parameters (S_a and S_q) were calculated according to the ISO 25178 standard [29]. The chemical composition of the surface was investigated using an X-ray photoelectron spectroscopy (XPS) apparatus (Axis Ultra DLD, Kratos Ltd., Manchester, UK). The characterization was performed using a monochromatic Al X-ray source. The water contact angles (CAs) of deionized water in a volume of approximately 15 μL were measured using a contact angle meter to study the wettability of the coatings. Drop images were recorded and analyzed using the image processing program ImageJ (Version 1.4.3.67), plug-in Dropsnake. The contour of the drop was then determined using the piecewise polynomial fitting method, and the CA was then calculated.

The elastic modulus of the coatings was measured using a compression test by a universal testing machine (INSTRON 4505, Norwood, MA, USA). The test samples were cylindrical (height: 50 mm, diameter: 30 mm) and made by the casting method. After curing, the cylindrical samples were mounted on the universal testing machine and tested with an indenter at a speed of 0.2 mm/min. The elastic modulus data were obtained from analyzing the displacement–load curve. The same three samples were prepared.

Coating adhesion testing was evaluated using an X-cut adhesion test in accordance with ASTM D3359 standard [30] (Method A). The methods of operation are as follows: An X-cut (~40 mm for an incision) is made through the film with a sharp razor blade tool to the substrate. Pressure-sensitive tape is applied over the cut. The tape is smoothed into place using a pencil eraser over the area of the incisions. The tape is removed by pulling it off rapidly back over itself as close to an angle of 180° as possible. There are six grades in the standard: 5A, 4A, 3A, 2A, 1A and 0A. Grade 5A indicates the highest adhesion, and 0A indicates the poorest adhesion.

The neutral salt spray aging test was performed using a salt spray tester (ASR-90A, Ledi Instrument Co., Ltd., Ningbo, China). An aqueous solution with a sodium chloride concentration of 50 g/L is prepared according to ASTM B117 standard [31], and the pH is controlled between 6.4 and 7.0. The temperature of the salt spray chamber is set at 35°C , and the salt spray volume is 1–2 mL/80 $\text{cm}^2\cdot\text{H}$. Four ratios of IPN gel coatings were selected for the test, and 70 specimens were produced for each ratio, for a total of 280 specimens. The total test time is 168 h. Every 12 h, five specimens of each ratio are removed from the salt spray tester, their ice adhesion strength is measured, and the average and standard deviation are calculated.

4. Results and Discussion

4.1. Icephobic Properties of the Epoxy/PDMS IPN Gel

The primary consideration in verifying the icephobic performance of a coating surface is its ice adhesion strength (τ_{ice}) [32]. In Figure 4, the τ_{ice} of PDMS gel coatings with varying silicone oil concentrations and epoxy/PDMS IPN gel coatings with different silicone oil concentrations are depicted at -10°C . Similar to previous measurements, the coating τ_{ice} increases with increasing epoxy content when the silicone oil content is constant [21]. The data also show that τ_{ice} decreases with increasing silicone oil content for PDMS gel, as well as for epoxy/PDMS IPN gel (1:1) and epoxy/PDMS IPN gel (2:1). When the silicone oil content was 200%, the τ_{ice} of the epoxy/PDMS IPN gel (1:1) was 8.4 ± 3.4 kPa. This value was similar to that of the pure PDMS gel with 200% silicone oil (6.5 ± 1.4 kPa). For comparison, the τ_{ice} of the pure epoxy coating was measured to be 282.1 ± 67.5 kPa. The above data show that epoxy/PDMS IPN gel (1:1) can be used as an icephobic coating that can remove ice under the action of natural forces. We are also curious as to what might be causing the above reduction in τ_{ice} .

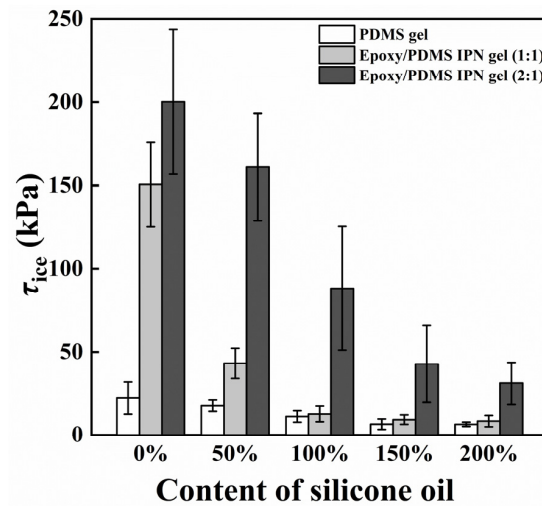


Figure 4. Content of silicone oil (% weight of PDMS) effect on ice adhesion strength τ_{ice} .

4.1.1. Surface Chemical Composition and Surface Topography

We want to understand the microstructure of the coating surface and try to answer the reasons for the above law of ice adhesion strength [22]. The chemical composition of the PDMS gel (200% content of silicone oil, the same below) and the epoxy/PDMS IPN gel (weight ratio of epoxy/PDMS = 1:1, 200% content of silicone oil, the same below) were analyzed with XPS. The wide-scan spectra of the PDMS gel and epoxy/PDMS IPN gel are shown in Figure 5a. The main chemical elements Si, C, and O were detected at approximately 98 eV, 280 eV and 528 eV for the two kinds of surfaces. The O, C, and Si atomic concentrations are approximately 22.57%, 55.53%, and 21.9%, respectively, for the PDMS gel. The O, C, and Si atomic concentrations are approximately 22.26%, 54.82%, and 22.92% for the epoxy/PDMS IPN gel. Thus, the atomic concentrations of the two kinds of surfaces are similar. The Si 2p, C 1s, and O 1s high-resolution XPS spectra of the two coatings are shown in Figure 5b–d, respectively. The peak of one element (Si 2p, C 1s, or O 1s) in the PDMS gel is similar to that of the epoxy/PDMS IPN gel. The epoxy did not obviously change the chemical composition of the PDMS gel surface. This may be because of surface migration in the curing processes: the $-CH_3$ groups of PDMS and silicone oil moved to the coating surface, thus decreasing the surface energy.

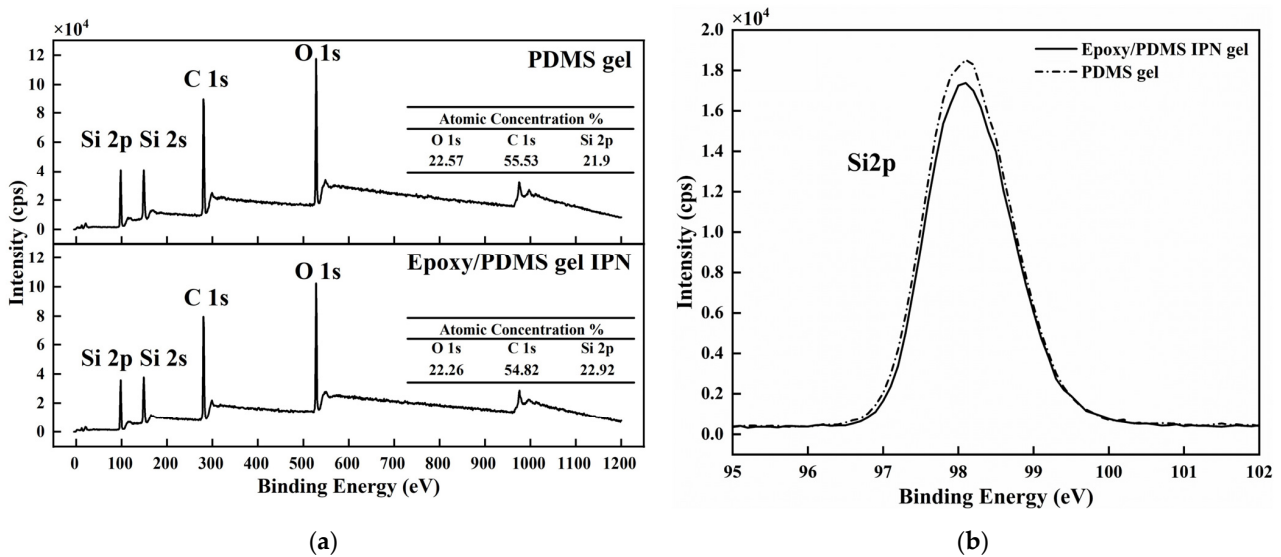


Figure 5. Cont.

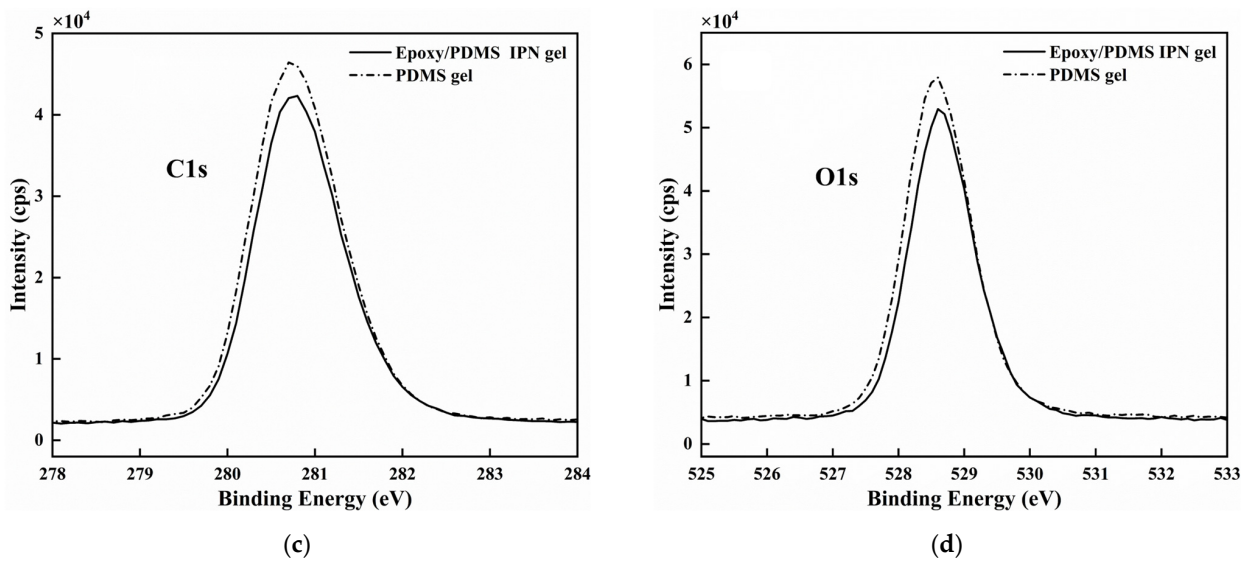


Figure 5. (a) The wide-scan XPS spectra of the PDMS gel and the epoxy/PDMS IPN gel. Atomic concentrations (%) of O, C, and Si are shown in the inset. High-resolution XPS spectra of (b) Si 2p, (c) C 1s, and (d) O 1s for the two coatings.

The surface morphology was obtained using an optical profilometer. Figure 6 shows the 3D morphology images and surface profile of the epoxy/PDMS IPN gel and PDMS gel. S_a and S_q were $0.776 \mu\text{m}$ and $0.975 \mu\text{m}$ for the epoxy/PDMS IPN gel, respectively. S_a and S_q were $0.264 \mu\text{m}$ and $0.342 \mu\text{m}$ for the PDMS gel. S_a and S_q parameters show that the epoxy/PDMS IPN gel has slightly more roughness than that of the PDMS gel surface. The R_a and R_q parameters also displayed similar characteristics. This is due to the chemical incompatibility between epoxy and PDMS at a microscopic level. However, it can be seen that the change in roughness is not the reason for the decrease in τ_{ice} of the epoxy/PDMS IPN gel.

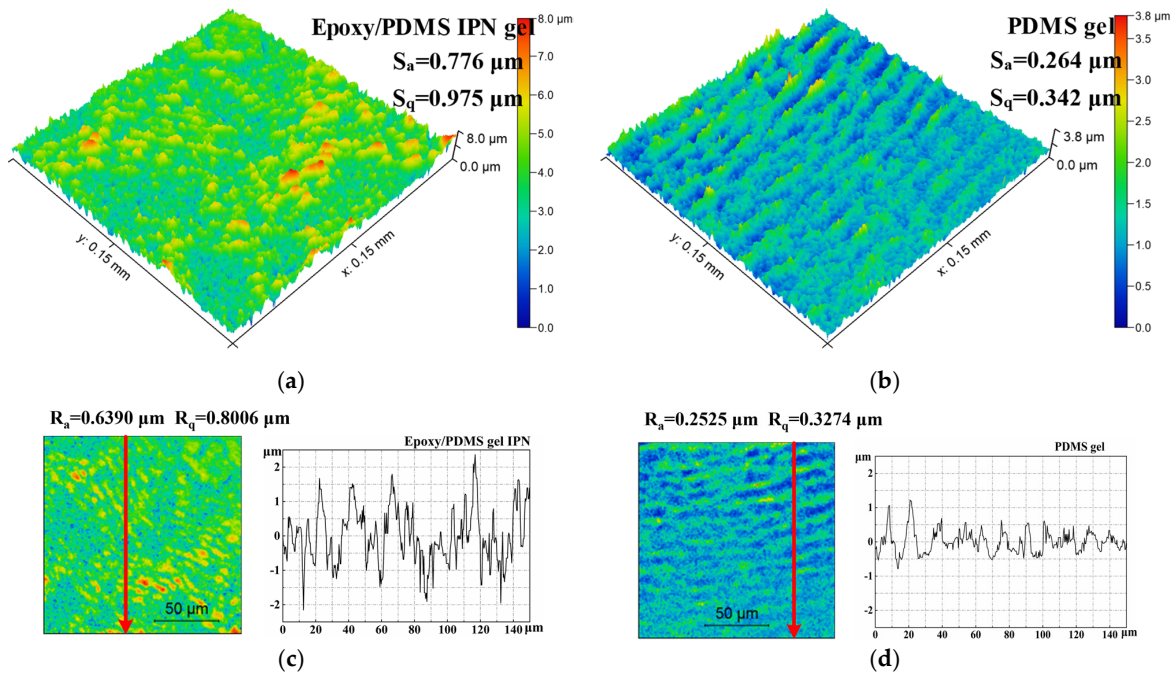


Figure 6. 3D optical profile images of (a) the epoxy/PDMS IPN gel and (b) PDMS gel. Scan size: $0.15 \text{ mm} \times 0.15 \text{ mm}$. Surface profiles of (c) the epoxy/PDMS IPN gel and (d) PDMS gel. The red arrows are the sampling paths for R_a and R_q .

4.1.2. Wettability

It is known that surface wettability can affect the ice adhesion strength [32]. To study the wettability of different surfaces, we measured the contact angle (CA) of the coating with the change in silicone oil content. In Figure 7, these samples had CAs ranging from 95° to 110°, which is similar to the previous measurements [33]. When the level of silicone oil was held constant, there was a decrease in CA with an increase in the level of epoxy. Additionally, with a high level of silicone oil, the decrease in the contact angle's trend slowed. The CA of the three coatings increased in a monotonic fashion with the increase in silicone oil content, indicating their hydrophobic nature due to the silicone components (PDMS and silicone oil). The order of CAs for the coatings is as follows: PDMS gel > epoxy/PDMS IPN gel (1:1) > epoxy/PDMS IPN gel (2:1). This is attributed to the epoxy component increasing the surface energy of the system. Overall, the CA of the epoxy/PDMS IPN gel (1:1) remains relatively constant and is not responsible for the observed decrease in τ_{ice} .

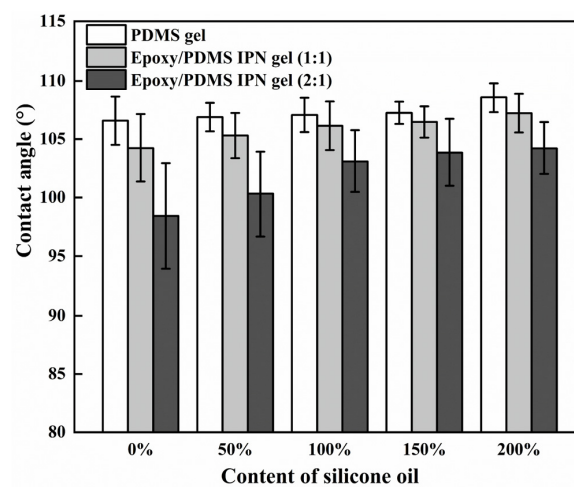


Figure 7. CA versus content of silicone oil (% weight of PDMS).

4.1.3. Elastic Modulus of the Epoxy/PDMS IPN Gel

To study the effect of changes in the mechanical properties of the coating on the icephobic properties, we measured the elastic modulus (E) [20]. Figure 8 shows the E of the epoxy/PDMS IPN gel coatings with various contents of silicone oil. The E value of the coatings decreased rapidly with increasing silicone oil content. This is because silicone oil reduces the crosslink density (ρ^{cl}) and reduces the stiffness ($G = RT\rho^{cl}$, where G is the shear modulus, T is the temperature in Kelvin, and R is the universal gas constant). Generally, the E value of pure epoxy is approximately 3–4 GPa [34]. Inversely, the E of the epoxy/PDMS IPN gel (1:1) with 200% silicone oil was only 0.18 MPa. This shows that the silicone oil significantly reduced the E value for the epoxy/PDMS IPN gel.

It can be observed from Figures 4 and 8, that τ_{ice} and E decreased simultaneously and significantly with increasing silicone oil content. Figure 9 shows the relationship between $E^{0.5}$ and τ_{ice} for (a) PDMS gel and the epoxy/PDMS IPN gel ((b) 1:1 and (c) 2:1). τ_{ice} shows a strong linear relationship with $E^{0.5}$ for the PDMS gel and epoxy/PDMS IPN gel (1:1). For the epoxy/PDMS IPN gel (2:1), τ_{ice} also shows a linear relationship with $E^{0.5}$ when $E^{0.5}$ is small (see red boxes in Figure 9c). This result was consistent with Equations (1) and (2) in Section 1, which showed that τ_{ice} is proportionate to $E^{0.5}$. In summary, the reduction in τ_{ice} is positively related to the modulus of the coating. The lower the elastic modulus, the lower the τ_{ice} . The mechanism of this phenomenon is considered from the perspective of fracture mechanics. Due to the low elastic modulus of the coating, when the ice cube is subjected to an external force, the soft coating can store more elastic strain energy, making it possible to detach the ice–coating interface. This provides a higher strain energy release rate for interface crack propagation. At the same time, due to the strong deformation ability of the soft coating, when the ice cube is subjected to external force, the ice–coating interface is more likely to cause local

debonding at the edge, resulting in a smaller debonding external force (ice adhesion strength). The research of He and Adja et al. [35,36] also verified this mechanism.

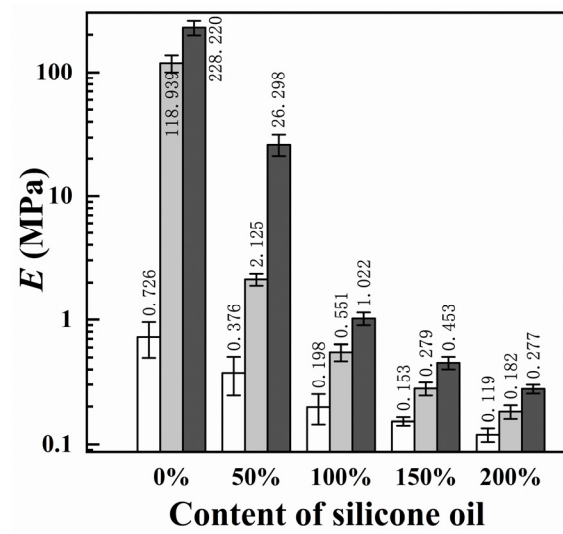


Figure 8. Content of silicone oil (% weight of PDMS) effect on elastic modulus E (semi-log plot).

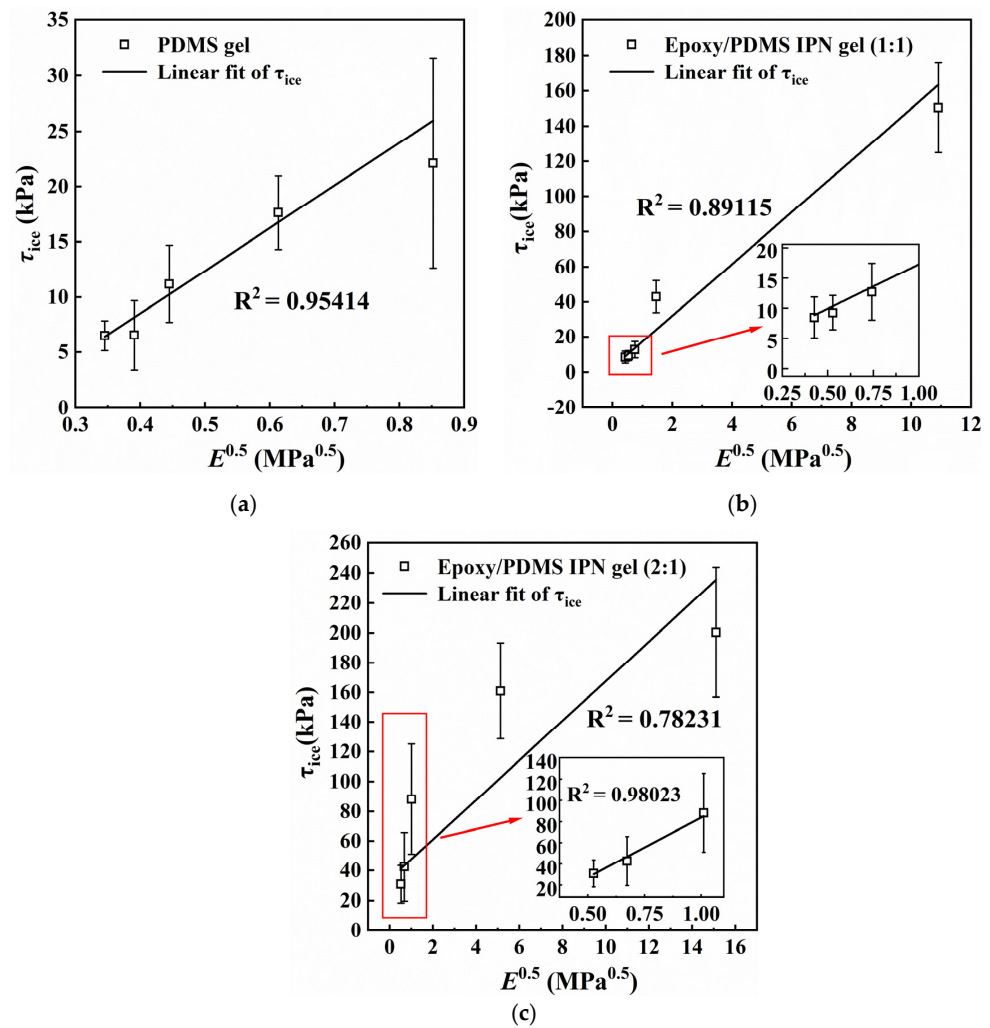


Figure 9. Relationship between $E^{0.5}$ and ice adhesion strength τ_{ice} for (a) PDMS gel, (b) epoxy/PDMS IPN gel (1:1), and (c) epoxy/PDMS IPN gel (2:1). Inset is the partial enlarged drawing.

4.2. Durability Test and Coating Adhesion Test

Durability and mechanical properties are important for icephobic coatings. A low elastic modulus means that a coating has poor strength [37]. A balance between icephobic properties and coating strength should be ensured. Therefore, icing/deicing cyclic tests, coating adhesion tests, and salt spray aging tests for the PDMS gel (200% content of silicone oil, the same below) and the epoxy/PDMS IPN gel (weight ratio of epoxy/PDMS = 1:1, 200% content of silicone oil, the same below) were carried out. At the same time, the salt spray aging test was performed on the two coatings without silicone oil as a control group. Deicing tests at different temperatures for the epoxy/PDMS IPN gel were carried out.

4.2.1. Icing/Deicing Cyclic Test

The icing/deicing cyclic test results are shown in Figure 10. In 25 icing/deicing cyclic tests, the τ_{ice} of epoxy/PDMS IPN gel coating was stable (within the range of 3–14 kPa). There were no visible cracks or flaking after 25 cyclic tests. This indicates that the durability of the epoxy/PDMS IPN gel is reliable. For the PDMS gel coating, debonding occurred after approximately seven cyclic tests.

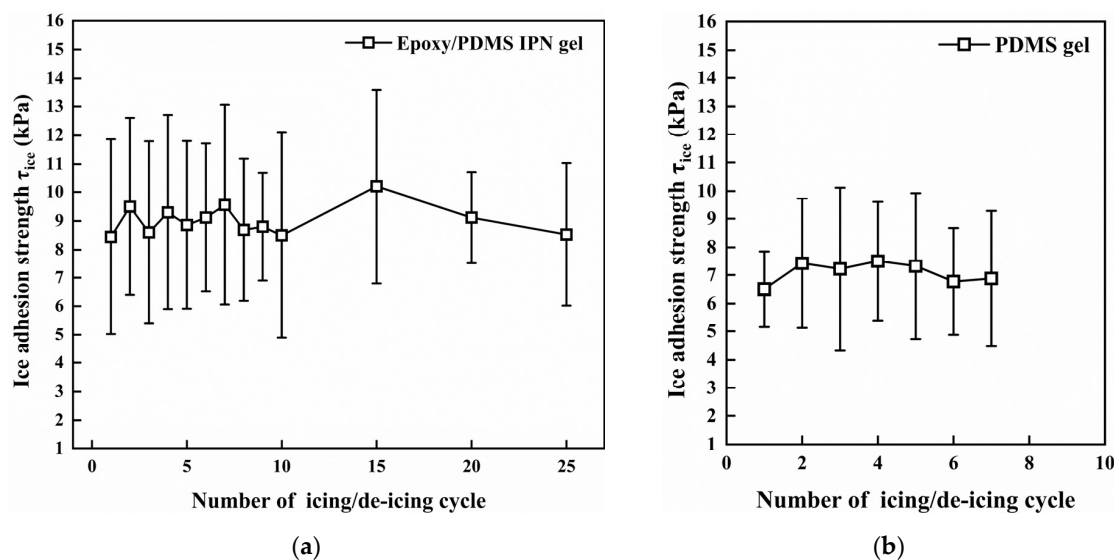


Figure 10. Icing/deicing cyclic tests for (a) epoxy/PDMS IPN gel and (b) PDMS gel coating ($-10\text{ }^{\circ}\text{C}$).

4.2.2. Deicing Tests at Different Temperatures

Since temperature is known to play an important role in the τ_{ice} of coatings, the τ_{ice} of the epoxy/PDMS IPN gel was tested at temperatures ranging from -5 to $-30\text{ }^{\circ}\text{C}$, shown in Figure 11. The τ_{ice} only slightly increased as the temperature decreased. When the temperature was $-30\text{ }^{\circ}\text{C}$, the τ_{ice} of the epoxy/PDMS IPN gel was only $14.3 \pm 5.8\text{ kPa}$. This may be due to the low melting point of silicone oil ($\sim -30\text{ }^{\circ}\text{C}$, PMX-200, -50 cs). The silicone oil molecules with low melting points were locked in the IPN network and ensured molecular flexibility of the coating at a low temperature, thus maintaining a low modulus and resulting in low τ_{ice} . The results show the practicality of the epoxy/PDMS IPN gel icephobic coating over a wide range of temperatures.

4.2.3. X-Cut Coating Adhesion Test

The coating adhesion test for the epoxy/PDMS IPN gel and PDMS gel coating were performed with an X-cut test (ASTM D3359, method A). There are six grades in the standard: 5A, 4A, 3A, 2A, 1A, and 0A. Grade 5A indicates the highest adhesion, and 0A indicates the poorest adhesion. Figure 12 shows the results of the X-cut adhesion test for the epoxy/PDMS IPN gel coating and PDMS gel coating. In Figure 12, there were many noticeable jagged cracks and small flakes along the X incision of the PDMS gel coating. Coating

debonding was also found. Thus, the PDMS gel coating was rated as 2A~3A according to ASTM D3359. However, for the epoxy/PDMS IPN gel coating and the epoxy/PDMS IPN gel coating for 25 icing/deicing cyclic tests, there were no noticeable jagged cracks or small chips along the X incision. It was rated as 5A according to the ASTM D3359. The epoxy/PDMS IPN gel coating showed better adhesion and mechanical properties than the PDMS gel coating.

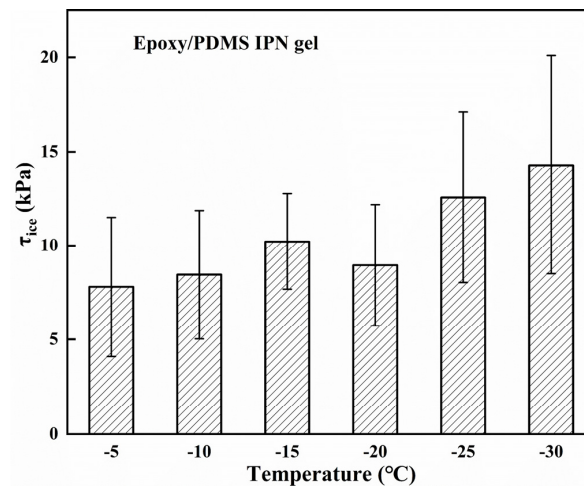


Figure 11. The ice adhesion strength τ_{ice} of the epoxy/PDMS IPN gel in the temperature range of -5 to -30 °C.

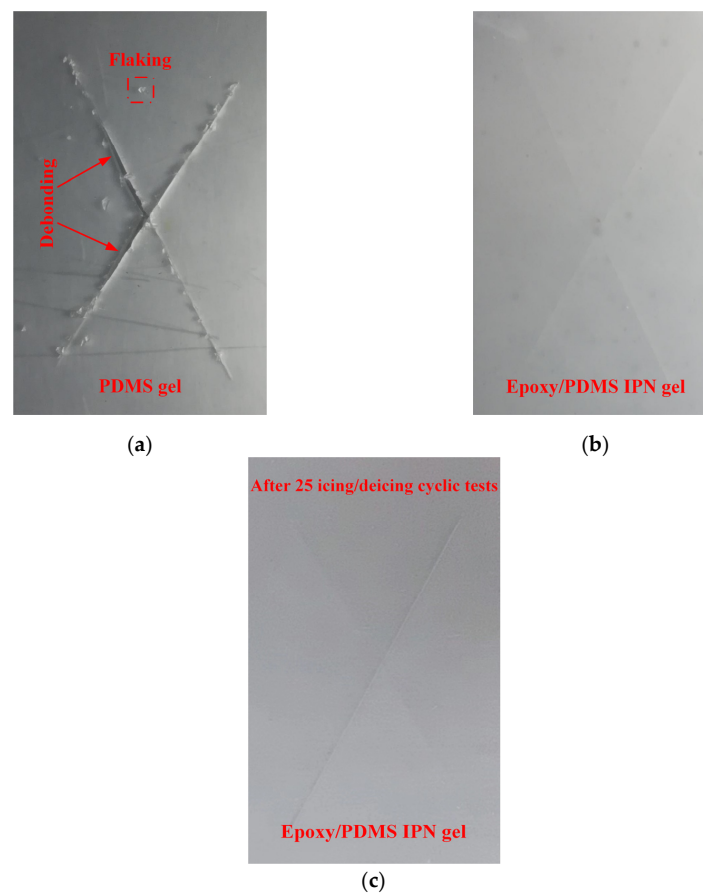


Figure 12. X-cut adhesion test for (a) PDMS gel, (b) epoxy/PDMS IPN gel, and (c) after 25 icing/deicing cyclic tests epoxy/PDMS IPN gel coatings.

4.2.4. Salt Spray Aging Test

Four coatings underwent the neutral salt spray aging test to determine the change in coating τ_{ice} over 168 h in a salt spray environment. The coatings tested were PDMS gel (0% and 200% content of silicone oil) and epoxy/PDMS IPN gel (weight ratio of epoxy/PDMS = 1:1, 0% and 200% content of silicone oil). The results are shown in Figure 13. We terminated the salt spray test when two types of PDMS gel coatings were slightly debonded after the test progressed to 168 h. The τ_{ice} of PDMS gel (0% content of silicone oil) and PDMS gel (200% content of silicone oil) increased slowly with time. At 144 h, the τ_{ice} of the two coatings reached their maximum values, which were 40.46 kPa and 32.13 kPa, respectively. Compared with their respective starting values, they increased by 18.34 kPa and 25.63 kPa, respectively, and the corresponding speed of increase was 0.1274 kPa/h and 0.1780 kPa/h. The τ_{ice} of the two coatings, epoxy/PDMS IPN gel (0% content of silicone oil) and epoxy/PDMS IPN gel (200% content of silicone oil), increased continuously, especially between 72 and 120 h, the τ_{ice} increased at a faster rate. The maximum value of ice-covered adhesion occurs at 168 h, with values of 186.11 kPa and 48.72 kPa for the two coatings, respectively, and corresponding growth rates of 0.2114 kPa/h and 0.2398 kPa/h. Based on the comparison of four coatings, we can note that coatings containing silicone oil show a faster increase in τ_{ice} and a greater decrease in icephobic ability during the salt spray aging test. The silicone oil migrates to the coating surface, making it susceptible to Cl^- corrosion in the salt spray test due to a Cl^- and $-OH$ displacement reaction [38]. From a results standpoint, the epoxy/PDMS IPN gel (200% content of silicone oil) was able to maintain an effective icephobic ability, with τ_{ice} at 48.72 ± 5.27 kPa even after 168 h of the salt spray aging test.

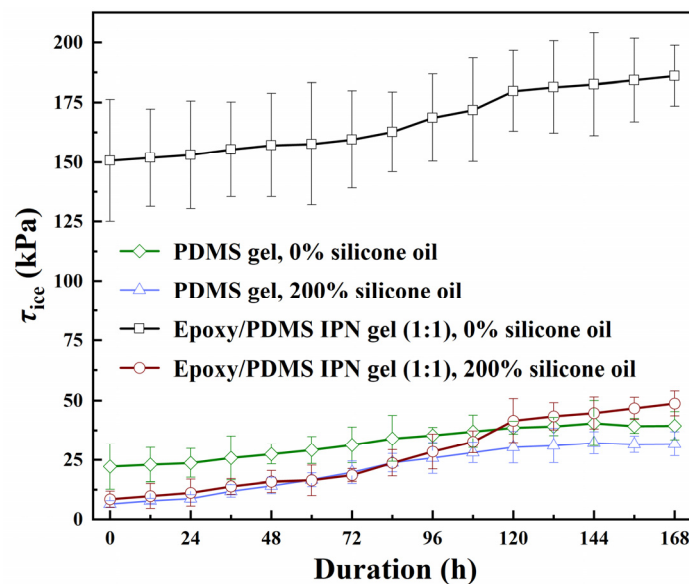


Figure 13. The ice adhesion strength τ_{ice} of the epoxy/PDMS IPN gel and PDMS gel coatings with the change in the coating duration of the neutral salt spray environment.

5. Conclusions

In this paper, we developed a durable icephobic coating utilizing a combination of epoxy, PDMS, and silicone oil via interpenetrating polymer network and gel techniques. We conducted tests on the durability and icephobic properties of the coating and arrived at the following conclusions.

- (1) The inclusion of silicone oil enhances the icephobic properties of the coating, addressing the previously identified lack of icephobic ability of the epoxy. At a 200% silicone oil content, the ice adhesion strength of the epoxy/PDMS IPN gel (1:1) measured 8.4 ± 3.4 kPa. Notably, there exists a strong linear relationship between τ_{ice} and

$E^{0.5}$. The roughness and wettability of the coating exhibit a negligible impact on its icephobic properties.

- (2) The epoxy/PDMS IPN gel (1:1) showed increased durability during icing/deicing cyclic tests and superior adhesion in X-cut coating adhesion tests. The ice adhesion strength of the epoxy/PDMS IPN gel (1:1) remained stable and below 20.1 kPa at temperatures ranging from -5 to -30 °C. Even after 168 h of the salt spray aging test, the epoxy/PDMS IPN gel (1:1) maintained an effective icephobic ability, with τ_{ice} at 48.72 ± 5.27 kPa.

The epoxy/PDMS IPN gel (1:1) shows low ice adhesion strength, high substrate adhesion, excellent weather resistance, and durability. This research not only provides guidance for the development of durable icephobic coatings but also inspires the creation of other protective coatings in road transportation, power industry, aerospace, wind power, ships, and ocean platforms to achieve high durability.

Author Contributions: L.Z.: conceptualization, methodology, investigation, validation, formal analysis, writing—original draft, writing—review and editing. T.H.: validation, writing—review and editing. Q.X.: investigation, validation. Y.T.: investigation, validation. J.Z.: supervision, writing—review and editing. H.G.: funding acquisition, project administration, writing—review and editing. All authors have read and agreed to the published version of the manuscript.

Funding: This research received no external funding.

Institutional Review Board Statement: Not applicable.

Informed Consent Statement: Not applicable.

Data Availability Statement: The data that support the findings of this study are available from the corresponding author, upon reasonable request.

Conflicts of Interest: The authors declare no conflicts of interest.

References

1. Golovin, K.; Tuteja, A. A Predictive Framework for the Design and Fabrication of Icephobic Polymers. *Sci. Adv.* **2017**, *3*, e1701617. [[CrossRef](#)] [[PubMed](#)]
2. Azimi Dijvejin, Z.; Jain, M.C.; Kozak, R.; Zarifi, M.H.; Golovin, K. Smart Low Interfacial Toughness Coatings for On-Demand de-Icing without Melting. *Nat. Commun.* **2022**, *13*, 5119. [[CrossRef](#)] [[PubMed](#)]
3. Esmeryan, K.D. From Extremely Water-Repellent Coatings to Passive Icing Protection-Principles, Limitations and Innovative Application Aspects. *Coatings* **2020**, *10*, 66. [[CrossRef](#)]
4. Zhu, Z.; Tian, Y.; Liu, Y.; Fu, K.; Chen, Q.; Zhang, B.; Zhang, H.; Zhang, Q. Facile Synthesis of Superhydrophobic Coating with Icing Delay Ability by the Self-Assembly of PVDF Clusters. *Colloids Surf. A Physicochem. Eng. Asp.* **2022**, *641*, 128562. [[CrossRef](#)]
5. Jian, Y.; Gao, H.; Yan, Y. Fabrication of a Superhydrophobic Micron-Nanoscale Hierarchical Structured Surface for Delayed Icing and Reduced Frosting. *Surf. Interfaces* **2022**, *34*, 102353. [[CrossRef](#)]
6. Zheng, Q.; Lv, J.; Zhang, J.; Feng, J. Fabrication and Application of Icephobic Silicone Coatings on Epoxy Substrate. *Prog. Org. Coat.* **2021**, *161*, 106483. [[CrossRef](#)]
7. Li, B.; Xiang, H.; Dai, X.; Zhu, T.; Hua, X.; Yuan, Y. A Superhydrophobic Anti-Icing Surface with a Honeycomb Nanopore Structure. *Coatings* **2023**, *13*, 1971. [[CrossRef](#)]
8. Yu, B.; Sun, Z.; Liu, Y.; Zhang, Z.; Wu, Y.; Zhou, F. Improving Anti-Icing and De-Icing Performances via Thermal-Regulation with Macroporous Xerogel. *ACS Appl. Mater. Interfaces* **2021**, *13*, 37609–37616. [[CrossRef](#)]
9. Golovin, K.; Kobaku, S.P.R.; Lee, D.H.; DiLoreto, E.T.; Mabry, J.M.; Tuteja, A. Designing Durable Icephobic Surfaces. *Sci. Adv.* **2016**, *2*, e1501496. [[CrossRef](#)]
10. Kim, J.H.; Kim, M.J.; Lee, B.; Chun, J.M.; Patil, V.; Kim, Y.-S. Durable Ice-Lubricating Surfaces Based on Polydimethylsiloxane Embedded Silicone Oil Infused Silica Aerogel. *Appl. Surf. Sci.* **2020**, *512*, 145728. [[CrossRef](#)]
11. Huang, X.; Tepylo, N.; Pommier-Budinger, V.; Budinger, M.; Bonaccorso, E.; Villedieu, P.; Bennani, L. A Survey of Icephobic Coatings and Their Potential Use in a Hybrid Coating/Active Ice Protection System for Aerospace Applications. *Prog. Aerosp. Sci.* **2019**, *105*, 74–97. [[CrossRef](#)]
12. Zarasvand, K.A.; Orchard, D.; Clark, C.; Golovin, K. Effect of Curvature on Durable Ice-Phobic Surfaces Based on Buckling Metallic Plates. *Mater. Des.* **2022**, *220*, 110884. [[CrossRef](#)]
13. Chatterjee, R.; Bararnia, H.; Anand, S. A Family of Frost-Resistant and Icephobic Coatings. *Adv. Mater.* **2022**, *34*, 2109930. [[CrossRef](#)] [[PubMed](#)]

14. Jeon, J.; Jang, H.; Chang, J.; Lee, K.-S.; Kim, D.R. Fabrication of Micro-Patterned Aluminum Surfaces for Low Ice Adhesion Strength. *Appl. Surf. Sci.* **2018**, *440*, 643–650. [[CrossRef](#)]
15. Hao, T.; Zhang, X.; Lei, Y.; Guo, H.; Zhang, J. Spontaneous Peeling of Ice Accretion: A Novel Expansion Force de-Icing Unit Based on Phase Transition Time Lag. *Cold Reg. Sci. Technol.* **2023**, *208*, 103801. [[CrossRef](#)]
16. Sethi, S.K.; Manik, G. A Combined Theoretical and Experimental Investigation on the Wettability of MWCNT Filled PVAc-g-PDMS Easy-Clean Coating. *Prog. Org. Coat.* **2021**, *151*, 106092. [[CrossRef](#)]
17. Zhuo, Y.; Xiao, S.; Amirfazli, A.; He, J.; Zhang, Z. Polysiloxane as Icephobic Materials—The Past, Present and the Future. *Chem. Eng. J.* **2021**, *405*, 127088. [[CrossRef](#)]
18. Liu, Y.; Zhao, Z.; Shao, Y.; Wang, Y.; Liu, B. Preparation of a Superhydrophobic Coating Based on Polysiloxane Modified SiO₂ and Study on Its Anti-Icing Performance. *Surf. Coat. Technol.* **2022**, *437*, 128359. [[CrossRef](#)]
19. Wang, X.; Huang, X.; Hu, W.; Ji, Z.; Sheng, H.; Liu, H. Fluorine-Free, Highly Transparent, Chemically Durable and Low Ice Adhesion Icephobic Coatings from Biobased Epoxy and Polydimethylsiloxane. *J. Appl. Polym. Sci.* **2023**, *140*, e53456. [[CrossRef](#)]
20. Qi, H.; Lei, X.; Gu, J.; Zhang, Y.; Gu, X.; Zhao, G.; Yu, J. Low Modulus of Polydimethylsiloxane Organogel Coatings Induced Low Ice Adhesion. *Prog. Org. Coat.* **2023**, *177*, 107435. [[CrossRef](#)]
21. Ziętkowska, K.; Kozera, R.; Przybyszewski, B.; Boczkowska, A.; Sztorch, B.; Pakuła, D.; Marciniec, B.; Przekop, R.E. Hydro- and Icephobic Properties and Durability of Epoxy Gelcoat Modified with Double-Functionalized Polysiloxanes. *Materials* **2023**, *16*, 875. [[CrossRef](#)] [[PubMed](#)]
22. Nosonovsky, M.; Hejazi, V. Why Superhydrophobic Surfaces Are Not Always Icephobic. *ACS Nano* **2012**, *6*, 8488–8491. [[CrossRef](#)] [[PubMed](#)]
23. He, Z.; Xiao, S.; Gao, H.; He, J.; Zhang, Z. Multiscale Crack Initiator Promoted Super-Low Ice Adhesion Surfaces. *Soft Matter* **2017**, *13*, 6562–6568. [[CrossRef](#)] [[PubMed](#)]
24. Jiang, X.; Lin, Y.; Xuan, X.; Zhuo, Y.; Wu, J.; He, J.; Du, X.; Zhang, Z.; Li, T. Stiffening Surface Lowers Ice Adhesion Strength by Stress Concentration Sites. *Colloids Surf. A Physicochem. Eng. Asp.* **2023**, *666*, 131334. [[CrossRef](#)]
25. Chaudhury, M.K.; Kim, K.H. Shear-Induced Adhesive Failure of a Rigid Slabin Contact with a Thin Confined Film. *Eur. Phys. J. E* **2007**, *23*, 175–183. [[CrossRef](#)] [[PubMed](#)]
26. Li, T.; Zhuo, Y.; Håkonsen, V.; He, J.; Zhang, Z. Durable Low Ice Adhesion Foams Modulated by Submicrometer Pores. *Ind. Eng. Chem. Res.* **2019**, *58*, 17776–17783. [[CrossRef](#)]
27. Ronneberg, S.; He, J.; Zhang, Z. The Need for Standards in Low Ice Adhesion Surface Research: A Critical Review. *J. Adhes. Sci. Technol.* **2020**, *34*, 319–347. [[CrossRef](#)]
28. Zheng, S.; Bellido-Aguilar, D.A.; Wu, X.; Zhan, X.; Huang, Y.; Zeng, X.; Zhang, Q.; Chen, Z. Durable Waterborne Hydrophobic Bio-Epoxy Coating with Improved Anti-Icing and Self-Cleaning Performance. *ACS Sustain. Chem. Eng.* **2019**, *7*, 641–649. [[CrossRef](#)]
29. ISO 25178; Geometrical Product Specifications (GPS)—Surface Texture: Areal. ISO: Geneva, Switzerland, 2017.
30. ASTM D3359; Standard Test Methods for Rating Adhesion by Tape Test. ASTM: West Conshohocken, PA, USA, 2017.
31. ASTM B117; Salt Spray Fog Testing. ASTM: West Conshohocken, PA, USA, 2019.
32. Zhuo, Y.; Håkonsen, V.; Liu, S.; Li, T.; Wang, F.; Luo, S.; Xiao, S.; He, J.; Zhang, Z. Ultra-Robust Icephobic Coatings with High Toughness, Strong Substrate Adhesion and Self-Healing Capability. *Sci. China Mater.* **2023**, *66*, 2071–2078. [[CrossRef](#)]
33. Bellido-Aguilar, D.A.; Zheng, S.; Huang, Y.; Zeng, X.; Zhang, Q.; Chen, Z. Solvent-Free Synthesis and Hydrophobization of Biobased Epoxy Coatings for Anti-Icing and Anticorrosion Applications. *ACS Sustain. Chem. Eng.* **2019**, *7*, 19131–19141. [[CrossRef](#)]
34. Yasmin, A.; Luo, J.J.; Abot, J.L.; Daniel, I.M. Mechanical and Thermal Behavior of Clay/Epoxy Nanocomposites. *Compos. Sci. Technol.* **2006**, *66*, 2415–2422. [[CrossRef](#)]
35. Adja, A.A.S.; Sobhani, S.; Momen, G.; Fofana, I.; Carrière, J. Step by Step Progress to Achieve an Icephobic Silicone-epoxy Hybrid Coating: Tailoring Matrix Composition and Additives. *J. Appl. Polym. Sci.* **2023**, *140*, e54262. [[CrossRef](#)]
36. He, Z.; Zhuo, Y.; Wang, F.; He, J.; Zhang, Z. Design and Preparation of Icephobic PDMS-Based Coatings by Introducing an Aqueous Lubricating Layer and Macro-Crack Initiators at the Ice-Substrate Interface. *Prog. Org. Coat.* **2020**, *147*, 105737. [[CrossRef](#)]
37. Stráský, J.; Preisler, D.; Seiner, H.; Bodnárová, L.; Janovská, M.; Košutová, T.; Harcuba, P.; Šalata, K.; Halmešová, K.; Džugan, J.; et al. Achieving High Strength and Low Elastic Modulus in Interstitial Biomedical Ti-Nb-Zr-O Alloys through Compositional Optimization. *Mater. Sci. Eng. A* **2022**, *839*, 142833. [[CrossRef](#)]
38. Ge, C.; Luo, X.; Wang, J.; Duan, J.; Wang, N.; Hou, B. Properties of KH550 and Hydroxyl Silicone Oil Co-modified Epoxy Resin and Its Mg-rich Primer. *J. Chin. Soc. Corros. Prot.* **2022**, *42*, 590–596.

Disclaimer/Publisher's Note: The statements, opinions and data contained in all publications are solely those of the individual author(s) and contributor(s) and not of MDPI and/or the editor(s). MDPI and/or the editor(s) disclaim responsibility for any injury to people or property resulting from any ideas, methods, instructions or products referred to in the content.